CFD Letters 14, Issue 7 (2022) 62-76

CFD Letters

Journal homepage:
https://semarakilmu.com.my/journals/index.php/CFD_Letters/index
ISSN: 2180-1363

Unsteady MHD on Convective Flow of a Newtonian Fluid Past an Inclined Plate in Presence of Chemical Reaction with Radiation Absorption and Dufour Effects

Obulesu Mopuri[1], Raghunath Kodi. Madhu[2], Mohan Reddy Peram[3], Charankumar Ganteda[4], Giulio Lorenzini[5,*], Nor Azwadi Che Sidik[6]

[1] Department of Mathematics, Siddharth Institute of Engineering &Technology (Autonomous), Puttur-517583, A.P., India
[2] Department of Humanities and Sciences, Bheema Institute of Technology and Science, Adoni-518301, Andhra Pradesh, India
[3] Department of Mathematics, Siddharth Institute of Engineering &Technology (Autonomous), Puttur-517583, A.P., India
[4] Department of Mathematics, Koneru Lakshmaiah Education Foundation, Vaddeswaram, Guntur, India
[5] University of Parma, Department of Engineering and Architecture, Parco Area delle Scienze 181/A, Parma 43124, Italy
[6] Malaysia – Japan International Institute of Technology (MJIIT), Universiti Teknologi Malaysia Kuala Lumpur, Jalan Sultan Yahya Petra (Jalan Semarak), 54100 Kuala Lumpur, Malaysia

ARTICLE INFO

Article history:
Received 16 June 2022
Received in revised form 24 June 2022
Accepted 3 July 2022
Available online 31 July 2022

Keywords:
Dufour effect; radiation absorption; MHD; porous medium; mixed convection; inclined plate

ABSTRACT

In this study, emission incorporation and Dufour belongings are investigated for uneven magnetohydrodynamic assorted convection stream over a disposed holey moving shield with thermal emission, heat assimilation, and homogenous substance reactions subjected to changeable suction. The governing momentum equation, as well as the energy and mass diffusion equations, have analytical solutions. The Nusselt number, the Sherwood number, in addition to velocity, temperature, attentiveness, and skin friction, are computed and examined analytically and visually in order to observe the manipulate of a variety of parameters. Grashof number (Gr), modified Grashof number (Gm), magnetic parameter (M), permeability parameter (K), Prandtl number (Pr), Heat Sink (Q), Radiation parameter (F), Dufour parameter (Du), Radiation absorption constraint (R), Schmidt number (Sc), and Chemical reaction parameter (K0) are all non-dimensional parameters with different values. In porous medium, slow-moving chemical reaction fluids are the only source of the issue. In the future, researchers may look at the inertia effects of porous medium for high-velocity flows. Researchers interested in radiation absorption effects in porous media will find this a highly helpful resource.

1. Introduction

The communication of fluid stream and captivating fields is the subject matter of magneto hydrodynamics. MHD authority generators, braking, plasma studies, petroleum industries, dimension of infusion flow rates in the food industry, cooling of nuclear reactors, space weather prediction, boundary-layer control in aerodynamics, and damping of turbulent fluctuations in

* *Corresponding author.*
E-mail address: giulio.lorenzini@unipr.it (Giulio Lorenzini)

https://doi.org/10.37934/cfdl.14.7.6276

semiconductor melts in crystal growth are all examples of magneto hydrodynamic flow of an electrically conducting fluid history a frenzied exterior.

Some early studies, for example Chen [1] and Chamkha *et al*., [2], investigated assorted convection stream in the forward stagnation area of a revolving sphere with unstable MHD heat and mass transfer at various wall conditions. In 2014, Raju *et al*., [3] considered the effect of viscous dissipation and joule's heating to study steady MHD forced convective flow of a viscous fluid of finite depth in a saturated porous medium over a fixed horizontal channel. Later, Sekhar *et al*., [4] analysed a semi-infinite semi-permeable vertical moving plate with a heat source and sink with an unstable MHD Casson fluid on the performance of heat and mass transfer. Animasaun [5] studied non-Darcian MHD free convective heat and mass transfer in dissipative Casson fluid flow with nth-order chemical reactions and suction in terms of thermal conductivity, variable viscosity, and thermophoresis. Obulesu *et al*., [6] analyzed radiation absorption effect on MHD dissipative fluid past a vertical porous plate embedded in porous media.

The effects of thermal diffusion and chemical reaction on MHD Casson fluid flow past a vertical porous plate have been investigated by Raghunath *et al*., [7]. A half-infinite porous plate with a chemically reacting and radiating fluid has been investigated for the convection flow effects of a magnetic field and radiation absorption by Obulesu *et al*., [8]. There has been discussion on the effect of Joule heating on MHD fluid flow past a vertical porous plate embedded in a porous medium by Obulesu *et al*., [9]. Pavan kumar *et al*., [10] modeled the effect of thermal diffusion and inclined magnetic fields on MHD free convection of Casson fluid past an inclined plate in a conducting field, Obulesu *et al*., [11] developed Effects of Hall current on convective flow past a porous plate with thermal radiation, chemical reaction, and thermophoresis. Vijaya *et al*., [12] studied a Casson fluid flow with contraction and expansion through a vertical porous channel is studied using radiation and Soret equations. Ramana Reddy *et al*., [13] conducted simulations of unsteady heat transfer MHD flow over a stretching surface with injection and suction. Raghunath [14] the MHD flow of second grade fluid over an infinite permeable plate embedded in a porous medium was discussed. Multiple variables effect on MHD transient flow past a plate was reported by Dastagiri *et al*., [15]. Raghunath *et al*., [16] included considered Heat and mass relocate on an unsteady MHD flow from side to side permeable middle flanked by two porous perpendicular dishes. Hall current effects on MHD convective flow past a porous plate with thermal radiation, chemical reaction with radiation absorption was discussed by Obulesu *et al*., [17]. Obulesu *et al*., [18] later developed MHD double diffusive visco-elastic fluid flow past an infinite vertical porous plate under the influence of radiation absorption.

The thermal dispersal (TD) procedure, as well recognized as the thermo unthinking deposition/diffusion (TRD) procedure and the Toyota dispersion development, is a high-temperature outside adjustment procedure that forms a hard, thin, wear-resistant deposit of carbides, nitrides, or carbonitrides on steels and other carbon-containing materials such as nickel and cobalt alloys, cemented carbides, and steel bonded carbides on steels (TiC dispersed in a steel matrix). When TD is used, the carbon and nitrogen diffuse into a layer of carbide-forming metals like vanadium, niobium, tantalum, chrome, molybdenum, or tungsten coated with such carbide-forming metals as vanadium, niobium, tantalum, chromium, or molybdenum. A nonporous, metallurgically bound layer will form on the substrate when the dispersed carbon or nitrogen interacts with the carbide- and nitride-forming components of the coating. Krishnamurthy *et al*., [19] stated that the MHD Double Diffusive method, based on Soret and Dufour, produces perpendicular wavy surfaces that are inserted into doubly stratified fluid-saturated porous media. Umamaheswar *et al*., [20] examined the chemical reaction effect on MHD double diffusive fluid flow over a rotating porous plate. Nagaraju *et al*., [21] studied MHD fluid with viscoelastic flow previous an never-ending at right angles shield in the existence of chemical reaction and radiation. Harinath reddy *et al*., [22] investigated the MHD twofold diffusive convective stream of heat generating liquid in the presence of Soret effect. Chandra reddy [23] discussed the Buoyancy effects on chemically reactive magneto Nano fluid past a moving vertical plate. Agarwall and Ahmed [24] studied MHD mass transfer flow past an inclined plate with variable temperature and plate velocity embedded in a porous medium. Raghunath [25] discussed Unsteady MHD oscillatory Casson fluid flow past an inclined vertical porous plate in the presence of chemical reaction with heat absorption and Soret effects. Ramachandra Reddy *et al*., [26] studied characteristics of MHD Casson fluid past an inclined porous plate. Obulesu*et al*., [27] Conducted a MHD heat and mass transfer study on the steady flow of a convective fluid through a porous plate in the presence of a diffusion thermo and aligned magnetic field. Obulesu *et al*., [28] developed MHD heat and mass transfer steady flow of aconvective fluid through a porous plate in the presences of multiple parameters.

In all of the foregoing studies, the impact of radiation absorption in the presence of a magnetic field, a chemical reaction, and a heat source/sink is not taken into account [29-32]. As a result, in this chapter, an attempt is made to address the concerns of radiation absorption and dufour effect in the presence of a magnetic field, chemical reaction, and heat source/sink. This topic is a follow-up to Venkteswara Raju, Bala Anki Reddy, and Suneetha's [25] study, which considers "Thermophoresis effects on a radiating inclined permeable moving plate in the presence of chemical reaction and heat absorption," but does not address radiation absorption. A regular perturbation technique is used to solve the governing equations. The effects of emerging parameters are studying through graphs and tables.

2. Formulation of the Problem

It is proposed that a gelatinous and incompressible electro-conducting fluid flows through a semi-infinite inclined sliding plate immersed in a porous medium in a two-dimensional MHD flow as shown in Figure 1. Combined with heat radiation, radiation absorption, and homogeneous chemical processes, a uniform transverse magnetic field B0 can be studied. It is unspecified that no practical electrical energy exists, implying that there is no electrical field. Induced magnetic fields and Hall effects are regarded as minimal since the applied magnetic field, Reynolds number and transverse magnetic field are so small. The y* axis is taken perpendicular to the flow and the x* axis is taken in the upward direction.

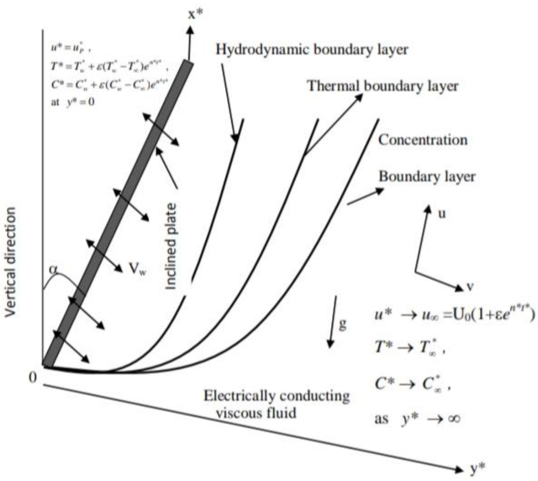

Fig. 1. Schematic diagram of the physical model and coordinate system

The shield is initially considered to move through a uniform rapidity u* in the liquid flow bearing, and the free of charge watercourse rapidity follows the exponentially growing small perturbation law. Aside from that, the warmth and attentiveness at the partition, in addition to the suction rapidity, are supposed to fluctuate exponentially with time.

The shield is initially considered to move through a uniform rapidity u* in the liquid flow bearing, and the free of charge watercourse rapidity follows the exponentially growing small perturbation law. Aside from that, the warmth and attentiveness at the partition, in addition to the suction rapidity, are supposed to fluctuate exponentially with time.

The governing equations are given by considering the preceding assumptions.

$$\frac{\partial v^*}{\partial y^*}=0 \tag{1}$$

$$\frac{\partial u^*}{\partial t^*}+V^*\frac{\partial u^*}{\partial y^*}=-\frac{1}{\rho}\frac{\partial p^*}{\partial x^*}+\vartheta\frac{\partial^2 u^*}{\partial y^{*2}}+g\beta_T(T^*-T_\infty^*)Cos\alpha+ + gB_C(C^*-C_\infty^*)Cos\alpha-\frac{\sigma B_0^2}{\rho}u^*-\frac{\vartheta u^*}{K^*} \tag{2}$$

$$\frac{\partial T^*}{\partial t^*}+V^*\frac{\partial T^*}{\partial y^*}=\frac{K}{\rho C_p}\frac{\partial^2 T^*}{\partial y^{*2}}-\frac{1}{\rho C_p}\frac{\partial q_r^*}{\partial y^*}-\frac{Q_1}{\rho C_p}\frac{\partial T^*}{\partial y^*} +\frac{R_1}{\rho C_p}(C^*-C_\infty^*)+\frac{DK_T}{C_s C_p}\frac{\partial^2 C^*}{\partial y^{*2}} \tag{3}$$

$$\frac{\partial C^*}{\partial t^*}+V^*\frac{\partial C^*}{\partial y^*}=D\frac{\partial^2 C^*}{\partial y^{*2}}-K_C(C^*-C_\infty^*) \tag{4}$$

The requisite border line circumstances for the distributions of rapidity, high temperature, and absorption under the preceding assumptions are given by

$$u^*=u_p^*,\quad T^*=T_w^*+\varepsilon(T_w^*-T_\infty^*)e^{n^*t^*},\ C^*=C_w^*+\varepsilon(C_w^*-C_\infty^*)e^{n^*t^*}\quad \text{at } y^*=0 \tag{5}$$

$$u^*\to u_\infty^*=U_0(1+\varepsilon e^{n^*t^*}),\quad T^*\to T_\infty^*\quad C^*\to C_\infty^*\quad \text{as}\quad y^*\to\infty \tag{6}$$

The suction velocity at the plate surface is just a function of time, as shown in Eq. (1), and it is assumed in the following form.

$$V^* = -V_0\,(1+\varepsilon A e^{nt}) \tag{7}$$

Eq. (8) changes beyond the boundary layer as

$$-\frac{1}{\rho}\frac{\partial p*}{\partial x*}=\frac{dU_\infty^*}{dt*}+\frac{\vartheta}{K^*}U_\infty^*+\frac{\sigma B_0^2}{\rho}U_\infty^* \tag{8}$$

We explore the following numerical representation for an optically thin boundary grey gas near stability:

$$\frac{\partial q_r*}{\partial y*}=4I(T*-T_w^*) \tag{9}$$

Where $I=\int_0^\infty K_{\lambda w}\left(\frac{\partial e_{b\lambda}}{\partial T}\right)_w d\lambda,$

$K_{\lambda w}$ is the incorporation coefficient at the wall and $e_{b\lambda}$ is the Planck`s function.

When the subsequent non-dimensional quantities are introduced,

$$u=\frac{u*}{U_0},\quad \vartheta=\frac{\vartheta*}{v_0},\quad y=\frac{v_0 y*}{\vartheta},\quad U_\infty=\frac{U_\infty^*}{U_0},\quad U_p=\frac{u_p^*}{U_0},\quad \theta=\frac{T*-T_\infty^*}{T_w^*-T_\infty^*},t=\frac{t*v_0^2}{\vartheta},$$
$$h=\frac{v_0L*}{\vartheta},\ C=\frac{C*-C_\infty^*}{C_w^*-C_\infty^*},\quad \Pr=\frac{\mu C_p}{K},\quad Sc=\frac{\vartheta}{D},\quad M=\frac{\sigma B_0^2\vartheta}{\rho v_0^2},K_C=\frac{\vartheta K_C^*}{v_0^2},\ n=\frac{n*v}{v_0^2},$$
$$F=\frac{4I_1\vartheta^2}{Kv_0^2},Q=\frac{Q_1}{\rho C_p v_0},Gr=\frac{\vartheta g\beta_T(T_w^*-T_\infty^*)}{U_0v_0^2},\quad Gm=\frac{\vartheta g\beta_c^{\,*}(C_w^*-C_\infty^*)}{U_0v_0^2},\quad K=\frac{v_0^2K*}{\vartheta^2},$$
$$Du=\frac{DK_T}{\upsilon C_sC_p}\frac{(C_w^*-C_\infty^*)}{(T_w^*-T_\infty^*)},\quad R=\frac{R_1\vartheta^2(C_w^*-C_\infty^*)}{Kv_0^2(T_w^*-T_\infty^*)}. \tag{10}$$

A non-dimensional recast of Eq. (2) to (4) can be obtained by using Eq. (7) to (9).

$$\frac{\partial u}{\partial t}-(1+\varepsilon Ae^{nt})\frac{\partial u}{\partial y}=\frac{dU_\infty}{dt}+\frac{\partial^2u}{\partial y^2}+GrCos\alpha\ \theta+GmCos\alpha\ C+N(U_\infty-u) \tag{11}$$

$$\Pr\frac{\partial\theta}{\partial t}-\Pr(1+\varepsilon Ae^{nt})\frac{\partial\theta}{\partial y}=\frac{\partial^2\theta}{\partial y^2}+\Pr Q\frac{\partial\theta}{\partial y}-\Pr F\theta+RC++\Pr Du\frac{\partial^2C}{\partial y^2} \tag{12}$$

$$Sc\frac{\partial C}{\partial t}-Sc(1+\varepsilon Ae^{nt})\frac{\partial C}{\partial y}=\frac{\partial^2C}{\partial y^2}-ScKcC \tag{13}$$

Where N=M+1/K

The connected border line surroundings are as follows:

$$u = U_p, \quad \theta = 1 + \varepsilon e^{nt}, \quad C = 1 + \varepsilon e^{nt}, \quad \text{at} \quad y = 0$$
$$u \to U_\infty = 1 + \varepsilon e^{nt}, \quad \theta \to 0, \quad C \to 0 \quad \text{as} \quad y \to \infty \tag{14}$$

3. Solution of the Problem

The partial differential Eq. (11) to (13) are linked non-linear partial differential equations that cannot be solved in closed form. These equations, on the other hand, may be reduced to a set of ordinary differential equations that can be solved numerically. So, this can be done, when the amplitude of oscillations (ε <<1) is very small.

The solutions of flow Velocity (u), Temperature field (), and Concentration(C) in the vicinity of the plate can be assumed to be as follows:

$$u(y,t) = u_0(y) + \varepsilon e^{nt} u_1(y)$$
$$\theta(y,t) = \theta_0(y) + \varepsilon e^{nt} \theta_1(y)$$
$$C(y,t) = C_0(y) + \varepsilon e^{nt} C_1(y) \tag{15}$$

The following equations are produced by substituting Eq. (15) into Eq. (11)–(13), equating the coefficients at the terms with the same powers of, and ignoring the terms of higher order.

Zeroth order:

$$u_0'' + u_0' - \mathrm{N}\ \mathrm{u}_0 = -\mathrm{N} - \mathrm{Gr}\ \mathrm{Cos}\,\alpha\ \theta_0 - \mathrm{Gm}\ \mathrm{Cos}\,\alpha\ C_0 \tag{16}$$

$$\theta_0'' + \Pr(1+Q)\theta_0' - \Pr \mathrm{F}\theta_0 = -\mathrm{R}C_0 - \Pr Du\, C_0'' \tag{17}$$

$$C_0'' + Sc\ C_0' - \mathrm{ScK}_C C_0 = 0 \tag{18}$$

First order:

$$u_1'' + u_1' - (\mathrm{N}+\mathrm{n})\mathrm{u}_1 = -(\mathrm{N}+\mathrm{n}) - \mathrm{A}u_0' - \mathrm{Gr}\ \mathrm{Cos}\,\alpha\ \theta_1 - \mathrm{Gm}\ \mathrm{Cos}\,\alpha\ C_1 \tag{19}$$

$$\theta_1'' + \Pr(1+Q)\theta_1' - \Pr(F + \mathrm{n})\ \theta_1 = -\Pr\mathrm{A}\theta_0' - \mathrm{RC}_1 - \Pr \mathrm{Du}\, \mathrm{C}_1'' \tag{20}$$

$$C_1'' + ScC_1' - Sc(Kc - n)C_1 = -\mathrm{ScA}C_0' \tag{21}$$

The associated boundary conditions are as follows:

$$u_0 = U_p, \quad u_1 = 0, \quad \theta_0 = 1, \quad \theta_1 = 1, \quad C_0 = 1, \quad C_1 = 1 \quad \text{at} \quad y = 0$$
$$u_0 = 1, \quad u_1 = 1, \quad \theta_0 \to 0, \quad \theta_1 \to 0, \quad C_0 \to 0, \quad C_1 \to 0 \quad \text{as} \quad y \to \infty \tag{22}$$

The following answers are derived by solving Eq. (16) – (21) under the boundary conditions Eq. (22).

$$C_0 = \exp(-m_1 y) \tag{23}$$

$$\theta_0 = b_1 \exp(-m_1 y) + b_2 \exp(-m_2 y) \tag{24}$$

$$u_0 = 1 + b_3 \exp(-m_1 y) + b_4 \exp(-m_2 y) + b_5 \exp(-m_3 y) \tag{25}$$

$$C_1 = b_6 \exp(-m_1 y) + b_7 \exp(-m_4 y) \tag{26}$$

$$\theta_1 = b_8 \exp(-m_1 y) + b_9 \exp(-m_2 y) + b_{10} \exp(-m_4 y) + b_{11} \exp(-m_5 y) \tag{27}$$

$$u_1 = 1 + b_{12} \exp(-m_1 y) + b_{13} \exp(-m_2 y) + b_{14} \exp(-m_3 y) + b_{15} \exp(-m_4 y) + b_{16} \exp(-m_5 y) + b_{17} \exp(-m_6 y) \tag{28}$$

We get the Velocity Temperature and Concentration field by substituting Eq. (23)–(28) in Eq. (15).

$$u = (1 + b_3 \exp(-m_1 y) + b_4 \exp(-m_2 y) + b_5 \exp(-m_3 y)) + + \varepsilon e^{nt} (1 + b_{12} \exp(-m_1 y) + b_{13} \exp(-m_2 y) + b_{14} \exp(-m_3 y) + + b_{15} \exp(-m_4 y) + b_{16} \exp(-m_5 y) + b_{17} \exp(-m_6 y)) \tag{29}$$

$$\theta = b_1 \exp(-m_1 y) + b_2 \exp(-m_2 y) + + \varepsilon e^{nt} (b_8 \exp(-m_1 y) + b_9 \exp(-m_2 y) + b_{10} \exp(-m_4 y) + + b_{11} \exp(-m_5 y)) \tag{30}$$

$$C = \exp(-m_1 y) + \varepsilon e^{nt} (b_6 \exp(-m_1 y) + b_7 \exp(-m_4 y)) \tag{31}$$

Skin Friction:

The friction coefficient at the surface of the skin is given by

$$\tau = \left(\frac{\partial u}{\partial y} \right)_{y=0}$$

$$\tau = -(m_1 b_3 + m_2 b_4 + m_3 b_5) - - \varepsilon (m_1 b_{12} + m_2 b_{13} + m_3 b_{14} + m_4 b_{15} + m_5 b_{16} + m_6 b_{17}) e^{nt} \tag{32}$$

Nusselt Number :

Temperature and Nusselt number determine the rate of heat transfer

$$Nu = -\left(\frac{\partial \theta}{\partial y} \right)_{y=0} \qquad Nu = (m_1 b_1 + m_2 b_2) + \varepsilon (m_1 b_8 + m_2 b_9 + m_4 b_{10} + m_5 b_{11}) e^{nt} \tag{33}$$

Sherwood Number :

According to Sherwood's number, the mass transfer rate on the wall is

$$Sh = -\left(\frac{\partial C}{\partial y} \right)_{y=0}$$

$$Sh = m_1 + \varepsilon (m_1 b_6 + m_4 b_7) e^{nt} \tag{34}$$

4. Result and Discussion

An analysis of the influence of various physical parameters, such as the Grashof number (Gr), the modified Grashof number (Gm), the magnetic parameter (M), the Permeability parameter (K), the Prandtl number (Pr), the Heat Sink (Q), Radiation parameter (F), Dufour parameter (Du), Schmidt number (Sc), and the Chemical reaction p on the dimensionless velocity fields, temperature fields, concentration fields, skin friction, Nusselt number, and Sherwood numbers will be Tables 1–3 indicate the effect of these factors on skin friction, Nusselt number, and Sherwood number.

Table 1
Skin Friction Variations

Gr	Gm	K	M	A	τ
5					3.9662
10					6.3009
15					8.6356
	6				4.2841
	12				6.1913
	18				8.0985
		1			3.9662
		2			4.3930
		3			4.5658
			2		3.9662
			3		3.3750
			4		2.9789
				π/6	6.8386
				π/4	5.5908
				π/3	3.9662

Provides numerical values for various Grashof numbers (Gr), modified Grashof numbers (Gm), magnetic parameters (M), porosity parameters (K), and inclined angle ().The Skin-friction increases with increased Grashof number (Gr), modified Grashof number (Gm), and Porosity parameter (K), while it decreases with increasing Magnetic parameter (M) and Inclined angle (I).

Table 2
Nusselt Number Variations

Pr	Q	F	R	Du	Nu
0.025					-4.4724
0.71					-1.1874
1					-0.5118
	1				-1.1874
	2				-1.0750
	3				-0.8299
		2			-0.0114
		4			1.1056
		6			1.7607
			1		0.2863
			3		-2.6611
			5		-5.6084
				2	-1.2757
				3	-1.3639
				6	-1.6288

Numbers for various Prandtl numbers (Pr), Radiation parameters (F), Heat source parameters (Q), and Radiation absorption values (R). Nusselt number increases as Prandtl number, Radiation parameter, and Heat source parameter increase, whereas it decreases as Radiation absorption parameter (R) and Dufour number (Du) increase.

Table 3
Sherwood Number Variation

Sc	Kc	Sh
0.22		0.2963
0.68		0.7727
1.25		1.3494
	3	0.9428
	5	1.1820
	6	1.2834

This table shows the Sherwood number (Sh) for the Schmidt number (Sc) and Chemical reaction parameter distinction values (Kc) .As shown in Table 3, the Sherwood number increases with increasing values of the Schmidt number and the Chemical reaction parameter.

Figures 2 and 3 show the influence of the Grashof number on the velocity profile for heat and mass transport when all other parameters are kept constant. The relative influence of the thermal buoyancy force on the viscous hydrodynamic force in the boundary layer is represented by the Grashof number for heat transmission. The increasing thermal buoyancy force causes an increase in velocity, as predicted. In addition, when Gr grows, the velocity near the porous plate rapidly climbs and then decays gradually to the free stream velocity. The relative influence of the thermal buoyancy force on the viscous hydrodynamic force in the boundary layer is represented by the Grashof number for heat transmission. The increasing thermal buoyancy force causes an increase in velocity, as predicted. In addition, when Gr grows, the velocity near the porous plate rapidly climbs and then decays gradually to the free stream velocity. The velocity distribution reaches a definite maximum value near the plate, then gradually drops to reach the free stream value. It is observed that as the Grashof number for mass transfer is increased, the velocity increases.

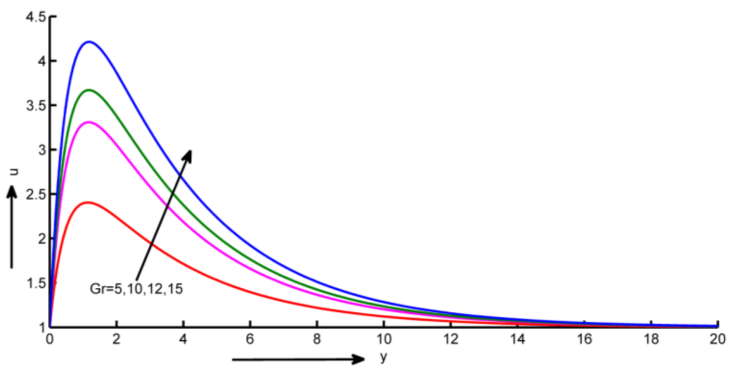

Fig. 2. The velocity profile for various Gr values

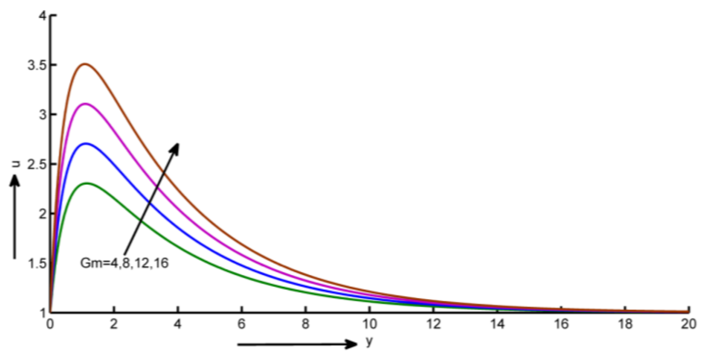

Fig. 3. The velocity profile for various Gm values

Figure 4 depicts the influence of the Hartmann number on velocity with a rise in the Hartmann number, the velocity falls. It's because the introduction of a transverse magnetic field produces a resistive type force (Lorentz force) that acts like a drag force, resisting fluid flow and lowering its velocity. In addition, when the Hartmann number rises, the thickness of the boundary layer decreases.

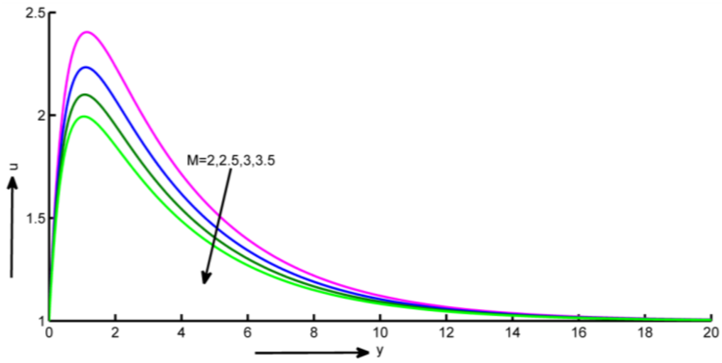

Fig. 4. The velocity profile for various M values

The influence of the permeability of the porous media parameter on the velocity distribution is shown in Figure 5. As can be seen, the velocity rises as the dimensionless porous media parameter rises. Physically, this outcome may be obtained by ignoring the holes in the porous substance.

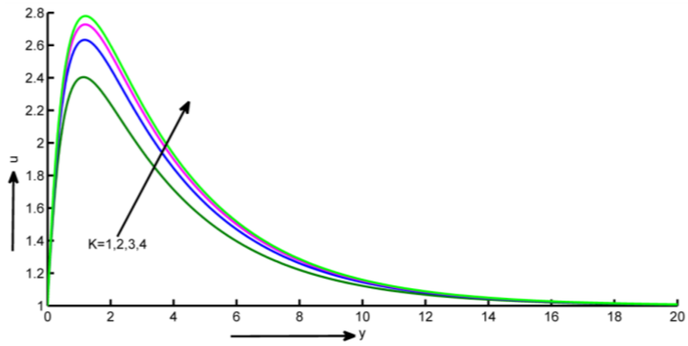

Fig. 5. The velocity profile for various K values

The effect of the angle of inclination parameter on velocity profiles is seen in Figure 6. We can see from this graph that the velocity profiles decrease when the angle of inclination parameter is increased.

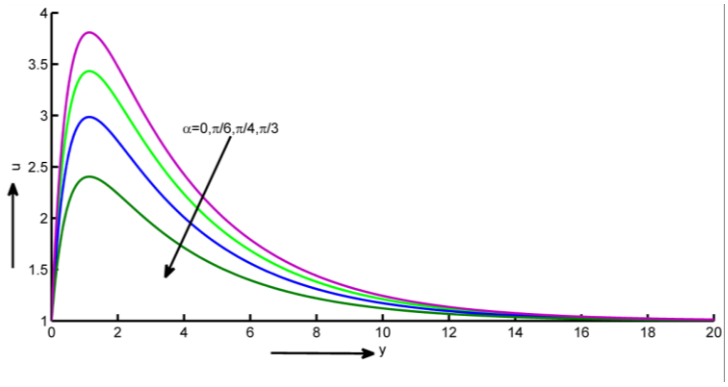

Fig. 6. For various values of, the velocity profile is shown

The influence of the Prandtl number on the temperature field is seen in Figure 7. Because either increases in kinematic viscosity or decreases in thermal conductivity lead to a rise in the Prandtl number, it is noticed that an increase in the Prandtl number leads to a drop in the temperature field. Hence temperature decreases with increasing of Prandtl number.

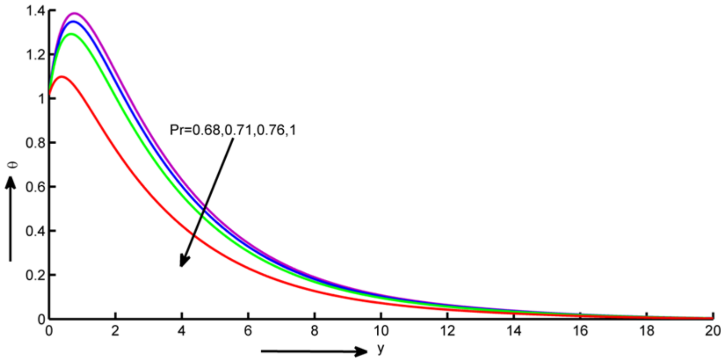

Fig. 7. The temperature profile for various Pr values

The effect of thermal radiation conduction on temperature is seen in Figure 8. It is obvious that when R increases, temperature decreases.

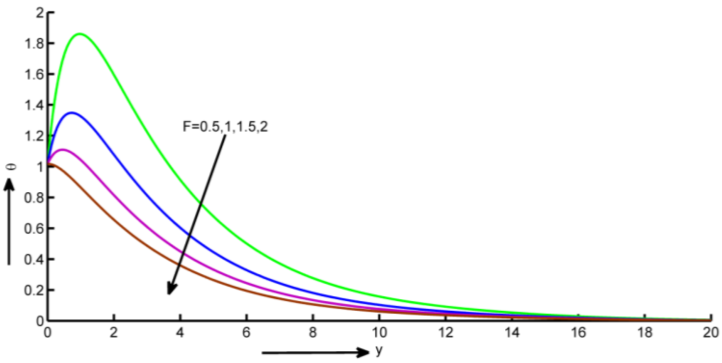

Fig. 8. For various values of F, the temperature curve is shown

Figures 9 and 10 show how the heat absorption coefficient Q affects temperature profiles. The existence of heat absorption (thermal sink) effects has the physical effect of lowering the fluid temperature. The thermal buoyancy effects are reduced as a result, resulting in a net drop in fluid temperature. As may be seen in Figs. 10 and 11, temperature distributions decrease as Q rises. It is also found that when the heat absorption effects rise, the thermal (temperature) boundary layer decreases.

Figure 10 shows the effect of the radiation absorption parameter on temperature. It is clear from these graphs that temperature rises as the radiation absorption parameter rises. Because thermal radiation is linked with high temperatures, the temperature distribution of the fluid flow is increased. Figure 11 shows a similar result when the Dufour number (Du) increases, which likewise raises the fluid temperature.

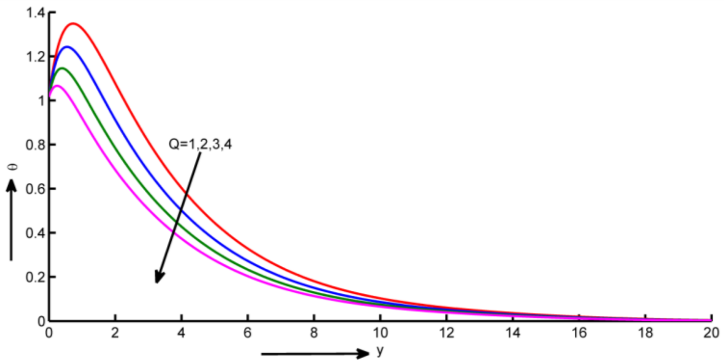

Fig. 9. For various values of Q, the temperature profile is shown

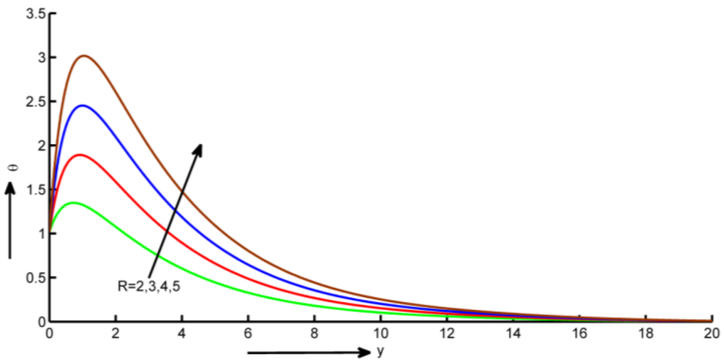

Fig. 10. For various R values, the temperature profile is shown

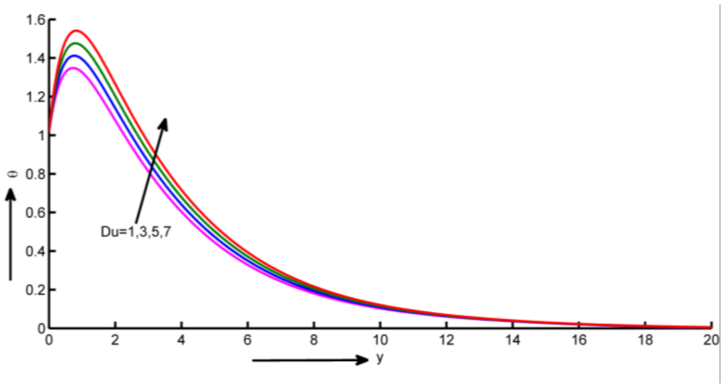

Fig. 11. The temperature profile for various Du values

Figure 12 depicts the effect of Schmidt number on concentration. It can be seen that concentration falls as the Schmidt number increases. Because the Schmidt number is a dimensionless number that is defined as the ratio of momentum and mass diffusivity and is used to characterise fluid flows that have both momentum and mass diffusion convection processes going on at the same time. When a result, as the Schmidt number rises, the concentration boundary layer shrinks.

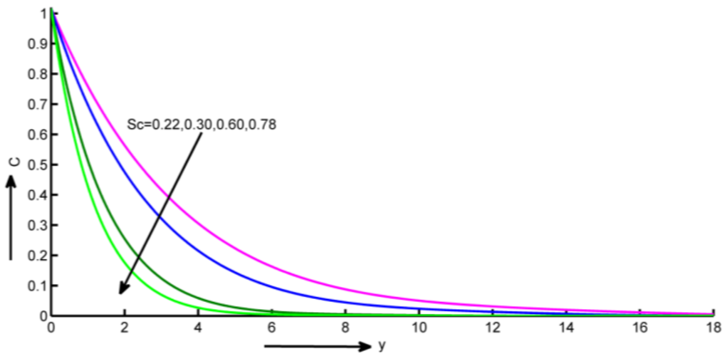

Fig. 12. For various levels of Sc, the concentration profile is shown

The effects of the chemical reaction parameter on the concentration profiles are shown in Figure 13. The concentration falls as the chemical reaction parameter Kc rises. As a result, the concentration buoyancy effects decrease, resulting in a drop in fluid concentration. Figure 13 depicts this tendency.

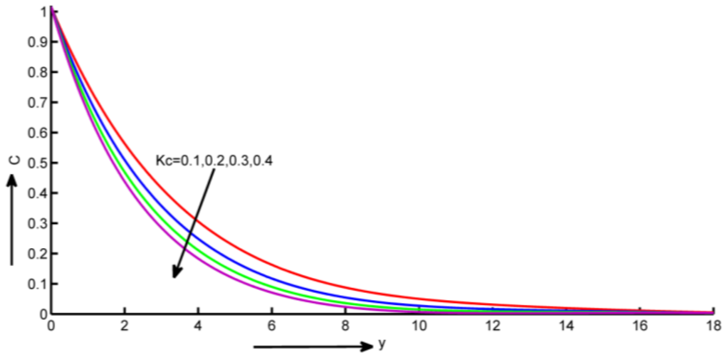

Fig. 13. The concentration profile for various Kc values

5. Conclusions

In this paper, we explored the trembling MHD on convective stream of a Newtonian fluid from side to side and disposed shield in the attendance of compound response, radiation absorption, and Dufour effects. The flow analysis yielded the following results.

I. Fluid velocity rises when the Grashof number and modified Grashof number rise, as does the porous medium's permeability parameter, but it decreases when the magnetic parameter and inclination angle are present.
II. Fluid temperature falls when Prandtl number, Radiation parameter, and Heat source restriction are in attendance, but it rises when Radiation absorption parameter and Dufour number are present.
III. Fluid deliberation decreases as the Schmidt number and substance response restriction rise.
IV. The permeability parameter (K), thermal Grashof number (Gr), and solutal Grashof number (Gm) all increased skin friction coefficient, whereas the magnetic field parameter (M) and inclination angle () decreased it.

V. The Nusselt number increases when the Prandtl number (Pr), heat absorption coefficient (Q), and Radiation parameter (F) rise, and lowers as the Dufour number (Du) and Radiation absorption parameter (F) grow (R).

VI. The mass transfer rate The Sherwood integer rises as the Schmidt number and chemical response restriction rise.

Acknowledgement
Authors would like to thank Universiti Teknologi Malaysia for the funding from Takasago TTES R.K130000.7843.4B732.

References

[1] Chen, C-H. "Heat and mass transfer in MHD flow by natural convection from a permeable, inclined surface with variable wall temperature and concentration." *Acta Mechanica* 172, no. 3 (2004): 219-235. https://doi.org/10.1007/s00707-004-0155-5

[2] Chamkha, Ali J., and Sameh E. Ahmed. "Unsteady MHD heat and mass transfer by mixed convection flow in the forward stagnation region of a rotating sphere at different wall conditions." *Chemical Engineering Communications* 199, no. 1 (2012): 122-141. https://doi.org/10.1080/00986445.2011.575907

[3] Raju, K. V. S., T. Sudhakar Reddy, M. C. Raju, PV Satya Narayana, and S. Venkataramana. "MHD convective flow through porous medium in a horizontal channel with insulated and impermeable bottom wall in the presence of viscous dissipation and Joule heating." *Ain Shams Engineering Journal* 5, no. 2 (2014): 543-551. https://doi.org/10.1016/j.asej.2013.10.007

[4] Kuppala, S. R., and G. Reddy Viswanatha. "Unsteady MHD convective heat and mass transfer of a casson fluid past a semi-infinite vertical permeable moving plate with heat source/sink." *Chemical and Process Engineering Research* 39 (2015): 5-12.

[5] Animasaun, I. L. "Effects of thermophoresis, variable viscosity and thermal conductivity on free convective heat and mass transfer of non-darcian MHD dissipative Casson fluid flow with suction and nth order of chemical reaction." *Journal of the Nigerian Mathematical Society* 34, no. 1 (2015): 11-31.

[6] Obulesu, M., and R. Siva Prasad. "Radiation Absorption Effect on MHD Dissipative Fluid Past A Vertical Porous Plate Embedded in Porous Media." *Bulletin of Pure & Applied Sciences-Mathematics and Statistics* 37, no. 1 (2018): 184-199. https://doi.org/10.5958/2320-3226.2018.00019.X

[7] Kodi, Raghunath, Obulesu Mopuri, Sujatha Sree, and Venkateswaraju Konduru. "Investigation of MHD Casson fluid flow past a vertical porous plate under the influence of thermal diffusion and chemical reaction." *Heat Transfer* 51, no. 1 (2022): 377-394. https://doi.org/10.1002/htj.22311

[8] Obulesu, M., and R. Siva Prasad. "Effect of Inclined Magnetic Field and Radiation Absorption on Mixed Convection Flow of a Chemically Reacting and Radiating Fluid Past a Semi Infinite Porous Plate." *i-Manager's Journal on Mathematics* 7, no. 4 (2018): 39. https://doi.org/10.26634/jmat.7.4.15561

[9] Obulesu, M., and R. Siva Prasad. "Joule Heating and Thermal Diffusion Effect on Mhd Fluid Flow Past a Vertical Porous Plate Embedded in a Porous Medium." (2019): 117-134. https://doi.org/10.5958/2320-3226.2019.00011.0

[10] Kumar, C. Pavan. "Thermal Diffusion And Inclined Magnetic Field Effects On Mhd Free Convection Flow Of Casson Fluid Past An Inclined Plate In Conducting Field." *Turkish Journal of Computer and Mathematics Education (TURCOMAT)* 12, no. 13 (2021): 960-977.

[11] Obulesu, M., K. Raghunath, and R. Sivaprasad. "Hall current effects on MHD convective flow past a porous plate with thermal radiation, chemical reaction with radiation absorption." In *AIP Conference Proceedings*, vol. 2246, no. 1, p. 020003. AIP Publishing LLC, 2020. https://doi.org/10.1063/5.0014423

[12] Vijaya, N., Y. Hari Krishna, K. Kalyani, and G. V. R. Reddy. "Soret and radiation effects on an unsteady flow of a casson fluid through porous vertical channel with expansion and contraction." *Frontiers in Heat and Mass Transfer (FHMT)* 11 (2018). https://doi.org/10.5098/hmt.11.19

[13] Reddy, G. Venkata Ramana, and Y. Hari Krishna. "Numerical solutions of unsteady MHD flow heat transfer over a stretching surface with suction or injection." *Fluid Dynamics and Materials Processing* 14, no. 3 (2018): 213-222.

[14] Raghunath, K., M. Obulesu, and A. Shareef. "MHD Flow of Second Grade Fluid over an Infinite Permeable Plate Embedded In a Porous Medium." *Journal of Xi'an University of Architecture & Technology* 12: 645-655.

[15] Dastagiri Y, Obulesu M, "Multiple variables effect on MHD transient flow past a plate." *Aegaeum Journal* (2020): 1276-1297

[16] Raghunath, K., M. Obulesu, and R. Sivaprasad. "Heat and mass transfer on an unsteady MHD flow through porous medium between two porous vertical plates." In *AIP Conference Proceedings*, vol. 2220, no. 1, p. 130003. AIP Publishing LLC, 2020. https://doi.org/10.1063/5.0001103
[17] Obulesu, M., K. Raghunath, and R. Sivaprasad. "Hall current effects on MHD convective flow past a porous plate with thermal radiation, chemical reaction with radiation absorption." In *AIP Conference Proceedings*, vol. 2246, no. 1, p. 020003. AIP Publishing LLC, 2020. https://doi.org/10.1063/5.0014423
[18] Damseh, Rebhi A., and B. A. Shannak. "Visco-elastic fluid flow past an infinite vertical porous plate in the presence of first-order chemical reaction." *Applied Mathematics and Mechanics* 31, no. 8 (2010): 955-962. https://doi.org/10.1007/s10483-010-1330-z
[19] Krishna Murthy and Vinay Kumar. "MHD Double Diffusive free convection process beside a perpendicular wavy surface implanted in a doubly stratified fluid-saturated porous medium under the inspiration of Soret and Dufour result." European Journal of Computational Mechanics 27, (2018). https://doi.org/10.1080/17797179.2018.1439150
[20] Umamaheswar, Raju, Varma, and Sucharitha "Chemical Reaction Effect On MHD Double Diffusive Fluid Flow Over A Rotating Porous Plate" *International Journal of Research -Granthaalayah* 2 (2017).
[21] Naga Raju, Hemalatha, Srihari Babu. "MHD fluid with viscoelastic flow bygone an infinite perpendicular plate in the existence of chemical reaction and radiation" *International journal of applied engineering research* 14(5) (2019).: 1062-1069,
[22] Reddy, Singamala Harinath, M. Umamaheswar, P. Chandra Reddy, M. C. Raju, and E. Keshava Reddy. "MHD double diffusive convective flow of heat generating fluid in the presence of Soret effect." In AIP Conference Proceedings, vol. 2246, no. 1, p. 020073. AIP Publishing LLC, 2020. https://doi.org/10.1063/5.0014623
[23] Chandra Reddy, P., K. Venkateswara Raju, M. Umamaheswar, and M. C. Raju. "Buoyancy effects on chemically reactive magnetonanofluid past a moving vertical plate." (2019): 193-207. https://doi.org/10.5958/2320-3226.2019.00017.1
[24] Agarwalla, Suman, and Nazibuddin Ahmed. "MHD mass transfer flow past an inclined plate with variable temperature and plate velocity embedded in a porous medium." *Heat Transfer—Asian Research* 47, no. 1 (2018): 27-41. https://doi.org/10.1002/htj.21288
[25] Kodi, Raghunath, and Obulesu Mopuri. "Unsteady MHD oscillatory Casson fluid flow past an inclined vertical porous plate in the presence of chemical reaction with heat absorption and Soret effects." *Heat Transfer* 51, no. 1 (2022): 733-752. https://doi.org/10.1002/htj.22327
[26] Vaddemani, Ramachandra Reddy, Raghunath Kodi, and Obulesu Mopuri. "Characteristics of MHD Casson fluid past an inclined vertical porous plate." *Materials Today: Proceedings* 49 (2022): 2136-2142. https://doi.org/10.1016/j.matpr.2021.08.328
[27] Mopuri, Obulesu, Raghunath Kodi, Charankumar Ganteda, Ramu Srikakulapu, and Giulio Lorenzini. "MHD heat and mass transfer steady flow of a convective fluid through a porous plate in the presence of diffusion thermo and aligned magnetic field." *Journal of Advanced Research in Fluid Mechanics and Thermal Sciences* 89, no. 1 (2022): 62-76. https://doi.org/10.37934/arfmts.89.1.6276
[28] Mopuri, Obulesu, Charankumar Ganteda, Bhagyashree Mahanta, and Giulio Lorenzini. "MHD heat and mass transfer steady flow of a convective fluid through a porous plate in the presence of multiple parameters." *Journal of Advanced Research in Fluid Mechanics and Thermal Sciences* 89, no. 2 (2022): 56-75. https://doi.org/10.37934/arfmts.89.2.5675
[29] Mahat, Rahimah, Muhammad Saqib, Imran Ulah, Sharidan Shafie, and Sharena Mohamad Isa. "MHD Mixed Convection of Viscoelastic Nanofluid Flow due to Constant Heat Flux." *Journal of Advanced Research in Numerical Heat Transfer* 9, no. 1 (2022): 19-25.
[30] Bakar, Fairul Naim Abu, and Siti Khuzaimah Soid. "MHD Stagnation-Point Flow and Heat Transfer Over an Exponentially Stretching/Shrinking Vertical Sheet in a Micropolar Fluid with a Buoyancy Effect." *Journal of Advanced Research in Numerical Heat Transfer* 8, no. 1 (2022): 50-55.
[31] Farahani, Somayeh Davoodabadi, Mahdi Alibeigi, and Hamed Hossienabadi Farahani. "The Uniform Magnetic Field Efficacy on Heat Transfer of Nanofluid Flow in A Flat Tube." *Journal of Advanced Research in Numerical Heat Transfer* 5, no. 1 (2021): 9-27.
[32] Khan, Ansab Azam, Khairy Zaimi, Suliadi Firdaus Sufahani, and Mohammad Ferdows. "MHD flow and heat transfer of double stratified micropolar fluid over a vertical permeable shrinking/stretching sheet with chemical reaction and heat source." *Journal of Advanced Research in Applied Sciences and Engineering Technology* 21, no. 1 (2020): 1-14. https://doi.org/10.37934/araset.21.1.114